



## Corrosion mechanisms of steel concrete moulds in the presence of a demoulding agent<sup>☆</sup>

A. CARNOT<sup>1,2</sup>, I. FRATEUR<sup>1,\*</sup>, P. MARCUS<sup>1</sup> and B. TRIBOLLET<sup>3</sup>

<sup>1</sup>Laboratoire de Physico-Chimie des Surfaces, CNRS (UMR7045), Ecole Nationale Supérieure de Chimie de Paris, 11 rue Pierre et Marie Curie, 75231 Paris Cedex 05, France

<sup>2</sup>CHRYSO, 7 rue de l'Europe, Z.I., 45300 Sermaises du Loiret, France

<sup>3</sup>Laboratoire de Physique des Liquides et Electrochimie, CNRS (UPR 15), Université Pierre et Marie Curie, 4 place Jussieu, 75252 Paris Cedex 05, France

(\*author for correspondence, Fax: +33 1 46 34 07 53, e-mail: ifrateur@ext.jussieu.fr)

Received 22 June 2001; accepted in revised form 12 March 2002

**Key words:** demoulding agent, EIS, filtered cement solution, mild steel, mortar, passivation

### Abstract

The behaviour of E24 mild steel, the constituent steel of most moulds for concrete, was studied by voltamperometry and electrochemical impedance spectroscopy in two electrolytes: (i) a filtered cement solution and (ii) a homogeneous mortar without large air cavities. Experiments were carried out with and without Aquadem<sup>®</sup>, a demoulding agent in aqueous phase. In the filtered cement solution, the E24 steel is passivated and the passivation mechanism is totally controlled by the anodic process, not by oxygen reduction. Whatever the experimental conditions (O<sub>2</sub> concentration, rotation speed, immersion time), the corrosion current,  $i_{\text{cor}}$ , is equal to the anodic plateau current and is of the order of  $0.8 \mu\text{A cm}^{-2}$ . Therefore  $i_{\text{cor}}$  can be directly assessed from the steady state current–potential curves. The E24 steel in contact with a homogeneous mortar without large air cavities is passivated as well as in the filtered cement solution. For both electrolytes, the results are independent of the presence or absence of Aquadem<sup>®</sup>. Therefore the pitting corrosion observed in service conditions does not arise from the presence of a solid phase in the electrolyte but may result from the heterogeneity of concrete created by air cavities.

### 1. Introduction

The corrosion of steel moulds used for prefabricated concrete is a phenomenon that is often encountered in the building industry. In general, the use of demoulding agents enables an easier demoulding of concrete, a better protection of moulds against corrosion [1] and a better cladding aspect of concrete pieces. However, Aquadem<sup>®</sup>, a demoulding agent in aqueous phase developed by CHRYSO, exhibits satisfactory properties except concerning protection against corrosion. Indeed, despite the action of concrete that, due to its high pH (around 13), leads to the formation of protective iron oxides [1], pitting corrosion of moulds is observed in the presence of Aquadem<sup>®</sup>. The corrosion products stain the concrete by encrustation. Therefore, the cladding aspect of these pieces is spoilt and the corroded moulds do not allow smooth concrete surfaces to be produced.

In contrast with the corrosion of reinforced concretes, which has been widely studied, that of steel moulds appears to be relatively unexplored topic. In reinforced

concretes, localized corrosion arises mainly from the presence of chloride ions and in this case, the diffusion of Cl<sup>-</sup> ions through concrete is the rate determining step [2–4]. For a better understanding of the corrosion mechanisms, the behaviour of E24 mild steel, the constituent steel of most moulds, was studied (i) in a filtered cement solution and (ii) in contact with a homogeneous mortar, with and without Aquadem<sup>®</sup> previously sprayed on the metal. Thus the behaviour of E24 steel was analysed in a liquid electrolyte (filtered cement solution) and in contact with a liquid/solid electrolyte (homogeneous mortar). For this purpose, several electrochemical techniques, such as voltamperometry and electrochemical impedance spectroscopy, were used.

### 2. Experimental details

All electrochemical measurements were performed with a three-electrode cell. The working electrode material was an E24 mild steel, according to the NF A 35-501 French standard, equivalent to a S235JR steel according to the EN 10025 European standard and to a A283C – A570Gr33 steel using the ASTM American codes. The

<sup>☆</sup>This paper was initially presented at the 5th International Symposium on Electrochemical Impedance Spectroscopy at Marilleva, Trento, Italy, June 2001.

main elements contained in such a material are: 0.18% C, 0.06% P and 0.05% S (mass ratios). All potentials were referred to a saturated sulfate electrode (SSE).

The experiments were carried out with or without Aquadem<sup>®</sup>, a molecule with phosphonate groups and a long alkyl chain [5]. For the experiments in the presence of the demoulding agent, the aqueous solution of Aquadem<sup>®</sup> (pH 7) was sprayed on the metal and let dry for 1 h in air, before putting the working electrode into contact with the electrolyte. The measurements were performed at room temperature.

A.c. impedance diagrams were collected by means of an Autolab PGSTAT30/FRA2 system from Eco Chemie; with a frequency domain ranging from 100 kHz to a few mHz and an amplitude of 10 mV.

### 2.1. Filtered cement solution

The working electrode was a rotating disc electrode (RDE) of 0.2 cm<sup>2</sup> surface area consisting of the cross-section of a cylindrical E24 steel rod, directly machined from a typical mould. The body of the rod was covered with cathaphoretic paint and then embedded in epoxy resin. Prior to any experiment, the electrode was mechanically polished with SiC paper down to grade 1200. The counter electrode was a platinum wire with a large area.

The electrolyte denoted 'filtered cement solution' was the aqueous phase collected by filtration of a Saint Pierre-la-Cour cement with a water/cement mass ratio equal to 0.5, 90 min after mixing. This homogeneous electrolyte was chosen because it was considered as representative of the liquid phase of concretes and suitable for laboratory experiments. Its pH was 13.1 and the concentrations of the main species contained in solution are given in Table 1.

Experiments were carried out in three solutions with different concentrations of dissolved oxygen: a deaerated solution obtained by nitrogen bubbling, an aerated solution in contact with the air, and a solution concentrated in oxygen by bubbling pure oxygen gas.

### 2.2. Mortar

The experimental set-up is presented in Figure 1. The working electrode was an E24 steel plate with only one side (12.25 cm<sup>2</sup> surface area) in contact with the mortar, the other sides being protected by cathaphoretic paint and epoxy resin. Prior to any experiment, the electrode was mechanically polished with SiC paper down to

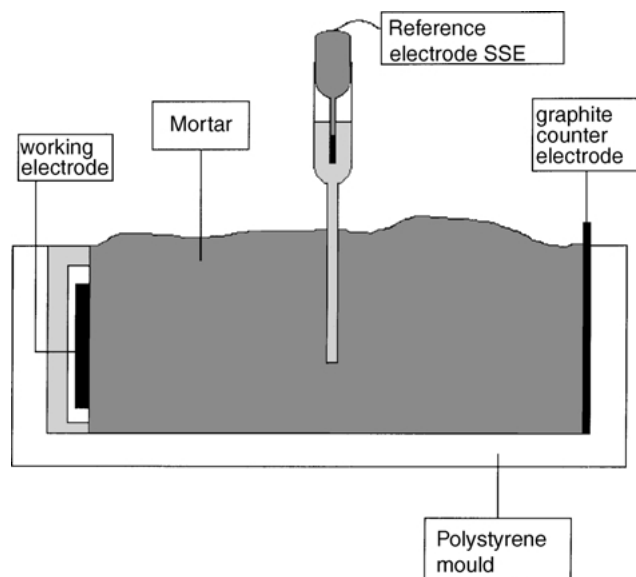


Fig. 1. Experimental set-up for experiments carried out with the steel surface in contact with the mortar.

grade 500. So as to avoid a distribution of potential at the surface of the working electrode, a large graphite sheet used as counter electrode was placed opposite the steel plate. The reference electrode (SSE) was in contact with the electrolyte through a glass extension directly set in the mortar.

The electrolyte was a mortar of normalised composition and with a water/cement mass ratio equal to 0.45. Thus it was possible to work for several hours (up to 8 h of setting) without encountering any difficulty of demoulding at the end of the experiment. Moreover, the conductivity of the mortar was high enough to plot current–potential curves or impedance diagrams.

During the mixing and the setting of the mortar, some air cavities, more or less numerous, and more or less large, were trapped in the electrolyte. However, the dimensions and the number of the cavities could be controlled. In the present work, only a homogeneous mortar without large air cavities was studied. Large cavities mean cavities of several millimetres diameter. Therefore, only the liquid/solid diphase electrolyte was considered (the gas–liquid–solid triphase electrolyte would be obtained by setting a mortar with large air cavities).

## 3. Results and discussion

### 3.1. Filtered cement solution

#### 3.1.1. Steady-state current–potential curves

Steady-state current–potential curves were plotted at zero rotation speed, for the three concentrations of dissolved oxygen (Figure 2(a) and (b)). In the present work, the curves are presented at zero rotation speed because, as discussed further, the rotation speed of the electrode,  $\Omega$ , has almost no influence on the results. The

Table 1. Concentrations of the main species contained in the filtered cement solution

Species	Ca <sup>2+</sup>	K <sup>+</sup>	Na <sup>+</sup>	SO <sub>4</sub> <sup>2-</sup>	OH <sup>-</sup>
Concentration/mmol L <sup>-1</sup>	15.38	202.62	55.28	80.79	127.08

Saint Pierre-la-Cour cement, water/cement mass ratio equal to 0.5, filtration 90 minutes after mixing.

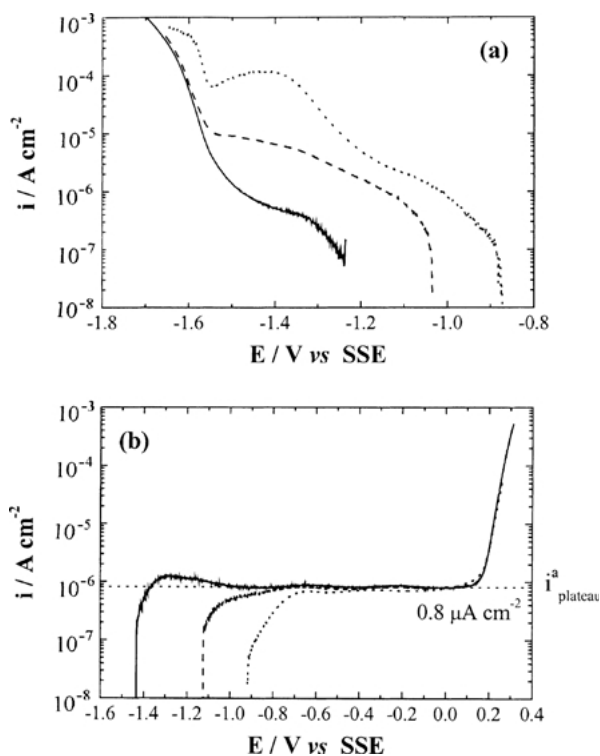


Fig. 2. Current-potential curves of an E24 steel RDE, with Aquadem<sup>®</sup> previously sprayed on the electrode, 1 h after immersion in a deaerated, aerated or concentrated in O<sub>2</sub> filtered cement solution, (a) Cathodic and (b) anodic curves.  $\Omega = 0$  rpm, sweep rate 0.1 mV s<sup>-1</sup>. Key: (—) N<sub>2</sub>, (---) air and (·····) O<sub>2</sub>.

anodic and cathodic curves were plotted separately, starting from the corrosion potential. The results are shown here with sprayed Aquadem<sup>®</sup>, but similar curves were obtained without Aquadem<sup>®</sup>.

First of all, it is observed that the higher the O<sub>2</sub> concentration, the higher the corrosion potential  $E_{\text{cor}}$ . In the anodic range and in the increasing potential direction, these curves show a wide current plateau  $i_{\text{plateau}}^{\text{a}}$  of the order of 0.8  $\mu\text{A cm}^{-2}$ , followed by a sharp increase of current corresponding to oxygen evolution. This anodic plateau is characteristic of a passive state of the electrode, corresponding to a limitation of current by mass transport through a compact oxide layer (e.g., by high-field migration [6]). The passivation of steel under these conditions is in agreement with the Pourbaix diagram for the iron-water system at 25 °C [7], which predicts that for a pH of 13.1 and a potential higher than -1.195 V vs SSE, the iron surface is covered by a Fe<sub>2</sub>O<sub>3</sub> layer.

It is important to notice that  $i_{\text{plateau}}^{\text{a}}$  (around 0.8  $\mu\text{A cm}^{-2}$ ) is independent of the oxygen concentration. Moreover, it is independent of (i) the rotation speed of the RDE, (ii) the immersion time of the electrode (between 0 and 24 h) and (iii) the presence or absence of Aquadem<sup>®</sup>.

In the cathodic region and in the decreasing potential direction, one or two current plateaux are observed (the second being around -1.5 V vs SSE), followed by a sharp increase in current corresponding to hydrogen

evolution. These cathodic plateaux, the heights of which increase with O<sub>2</sub> concentration, are assigned to dissolved oxygen reduction.

The shape of the cathodic curves is similar to that corresponding to 'classical' oxygen reduction on a uniformly reactive surface, limited by diffusion in solution or through a porous layer. However, the cathodic curves were plotted for different rotation speeds  $\Omega$  of the RDE and first, almost no influence of  $\Omega$  was noticed in the whole potential range, and second, the cathodic plateau currents are much smaller than the theoretical Levich currents [8] (the Levich currents are between 5 and 18 times higher than the experimental ones). Thus, despite the shape of the cathodic curves, the reduction of oxygen is not a simple reaction on a uniformly accessible metallic surface but rather a very complex mechanism via a compact passive layer.

Much work has been carried out to elucidate the oxygen reduction mechanism on passive films developed on iron or steel and in different electrolytes [9, 10]. However the cathodic reaction was not further investigated, as it was not the aim of the present paper.

Finally, these results indicate that a passive film covers the steel surface even at high cathodic potentials. The existence of a stable passive layer can be considered at least down to the corrosion potential measured in the deaerated solution, which is about -1.2 V vs SSE (Figure 2(a)). This value corresponds to the limit of the passive domain at pH 13.1 in Pourbaix diagram [7]. But during cathodic polarization below -1.2 V vs SSE, changes in the chemical state of iron cannot be excluded. Indeed, on passivated surfaces, O<sub>2</sub> reduction can occur simultaneously with the reduction of ferric oxide [9–11].

### 3.1.2. A.c. impedance diagrams

Figure 3 shows impedance diagrams plotted at  $E_{\text{cor}}$ , after 1 h of immersion in a deaerated, aerated or concentrated in O<sub>2</sub> solution, without Aquadem<sup>®</sup>. Similar results were obtained with Aquadem<sup>®</sup>. The impedance diagrams show a single capacitive loop with a large diameter (of the order of several hundreds of k $\Omega$  cm<sup>2</sup>) and independent of the oxygen concentration.

Impedance diagrams were also plotted at anodic potentials, from  $E_{\text{cor}}$  up to the anodic current plateau (i.e., up to 0 V vs SSE), in an aerated solution, and without Aquadem<sup>®</sup> (Figure 4). Again, similar results were obtained with Aquadem<sup>®</sup>. It is observed that, whatever the applied anodic potential, the diagrams are similar to that obtained at  $E_{\text{cor}}$ .

A rough calculation of the capacitance in function of the frequency, assuming a perfect half-circle (i.e., a single R/C parallel arrangement), gives values varying between 10  $\mu\text{F cm}^{-2}$  in the high frequency range and 50  $\mu\text{F cm}^{-2}$  in the low frequency range. This suggests that the electrical equivalent circuit for the steel/filtered cement solution interface is composed of two R/C parallel arrangements with close time constants: one relative to the charge transfer process (charge transfer

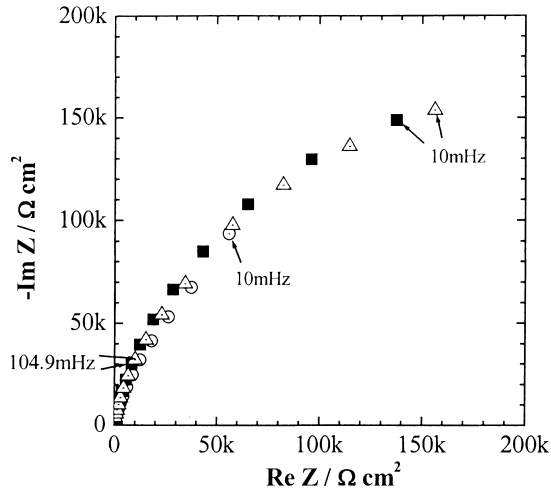


Fig. 3. A.c. impedance diagrams of an E24 steel RDE, plotted at  $E_{\text{cor}}$  after 1 h of immersion in a deaerated, aerated or concentrated in  $\text{O}_2$  filtered cement solution, without Aquadem<sup>®</sup>, and at 0 rpm. Key: (○)  $\text{N}_2$ , (■) air and (△)  $\text{O}_2$ .

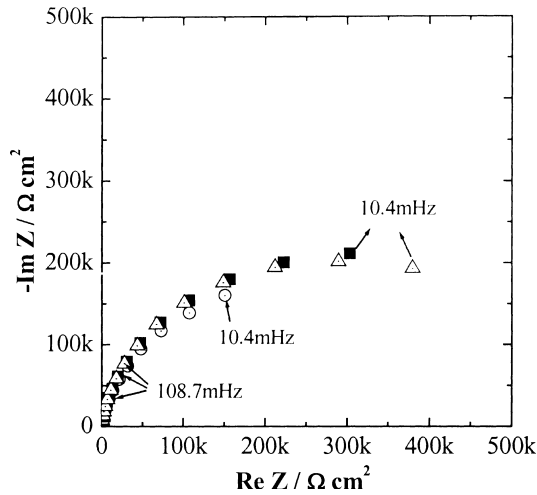


Fig. 4. A.c. impedance diagrams of an E24 steel RDE, plotted at  $E_{\text{cor}}$  and on the anodic plateau, after 1 h of immersion in an aerated filtered cement solution, without Aquadem<sup>®</sup>, and at 0 rpm. Key: (○)  $E_{\text{cor}}$ , (■)  $-0.4$  V and (△)  $-0.2$  V.

resistance in parallel with a double layer capacitance) and the other one to the passive film (film resistance in parallel with a film capacitance  $C_f$ ).

The film capacitance  $C_f$  can be assessed from the imaginary part of the impedance, by application of the relation:  $C_f = -1/(2\pi f \times \text{Im} Z)$  in the high frequency range. The mean values for  $C_f$ , calculated between 100 kHz and 20 kHz, are summarized in Table 2 as a function of dissolved oxygen concentration and applied potential.

As  $C_f$  is inversely proportional to the film thickness,  $x$ , according to  $C_f = \epsilon\epsilon_0/x$ , where  $\epsilon$  is the dielectric constant of the oxide covering the steel surface ( $\text{Fe}_2\text{O}_3$ ), a value of about  $10 \mu\text{F cm}^{-2}$  for  $C_f$  corresponds to a film thickness in the nanometer range. Such a small value for  $x$  is in agreement with the visual aspect of the electrode and may originate from the complex chemical composition of the solution (not only from the pH).

Table 2. Film capacitances calculated from the high frequency part of the impedance diagrams, as a function of the electrolyte, the dissolved oxygen concentration and the applied potential

Electrolyte	Filtered cement solution				Mortar	
	$\text{N}_2$	Air	Air	Air	$\text{O}_2$	Air
$E/\text{V vs SSE}$	$E_{\text{cor}}$	$E_{\text{cor}}$	$-0.4$	$-0.2$	$E_{\text{cor}}$	$E_{\text{cor}}$
$C_f/\mu\text{F cm}^{-2}$	12.2	11.8	9.0	7.5	10.0	0.5

Moreover,  $C_f$  decreases slightly when the  $\text{O}_2$  concentration increases and becomes smaller for more anodic applied potentials. Thus, the passive layer would be thicker for higher  $\text{O}_2$  concentrations and for higher anodic potentials. This may explain the shift observed in the low frequency range in Figures 3 and 4.

### 3.1.3. Discussion

In the filtered cement solution, the E24 steel is passivated at the corrosion potential, with or without sprayed Aquadem<sup>®</sup>. The above results show that, whatever (i) the rotation speed of the RDE, (ii) the dissolved oxygen concentration of the solution and (iii) the presence or the absence of Aquadem<sup>®</sup>, the anodic plateau current  $i_{\text{plateau}}^a$  is constant and of the order of  $0.8 \mu\text{A cm}^{-2}$  and the impedance diagrams plotted at  $E_{\text{cor}}$  are similar. Moreover, the impedance response is roughly independent of the applied anodic potential.

Therefore, the passivation of the E24 steel in the filtered cement solution is totally limited by the anodic process and not by the oxygen reduction. Thus the anodic current plateau can be extended down to  $E_{\text{cor}}$  and the current decrease observed between the beginning of the anodic plateau current and  $E_{\text{cor}}$  arises from the sum of the cathodic half-curve and the anodic plateau.

So the corrosion current  $i_{\text{cor}}$  is equal to  $i_{\text{plateau}}^a$ , and the total impedance of the electrode, that can be represented near  $E_{\text{cor}}$  by an anodic impedance,  $Z_a$ , in parallel with a cathodic impedance,  $Z_c$ , is equivalent to the single anodic impedance whatever the applied potential. This means that  $Z_c$  is much higher than  $Z_a$ , which is in agreement with the very small currents measured in the cathodic range (in comparison with Levich currents). This corroborates the presence of a compact passive layer at least down to  $-1.2$  V vs SSE [7]. However, during cathodic polarization below  $-1.2$  V vs SSE, a modification of the composition of this passive film cannot be excluded [9–11].

Finally, in this liquid electrolyte, the pitting corrosion observed in service conditions is not reproduced.

### 3.2. Mortar

The behaviour of E24 steel was studied in contact with a homogeneous mortar poured without formation of large air cavities (liquid–solid diphase electrolyte).

Anodic steady-state current–potential curves and impedance diagrams at  $E_{\text{cor}}$  were plotted after 1 h of

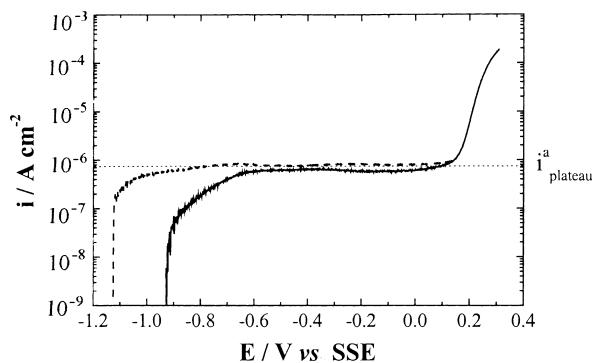


Fig. 5. Anodic current–potential curves of (—) an E24 steel plate, after 1 h of contact with a mortar poured without air cavity and (---) an E24 steel RDE at 0 rpm, after 1 h of immersion in an aerated filtered cement solution (with Aquadem<sup>®</sup>, sweep rate 0.1 mV s<sup>-1</sup>).

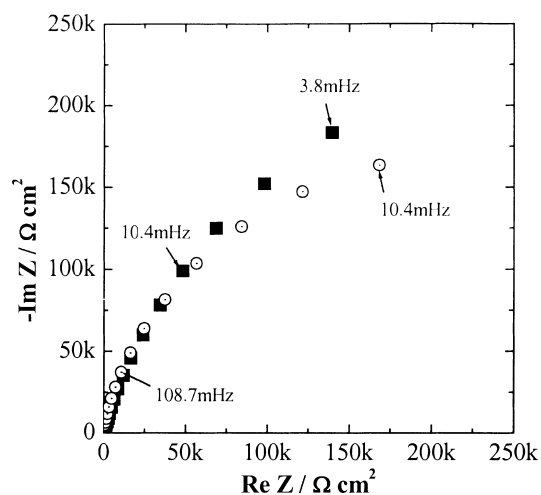


Fig. 6. A.c. impedance diagrams of (■) an E24 steel plate, after 1 h of contact with a mortar poured without air cavity and (○) an E24 steel RDE at 0 rpm, after 1 h of immersion in an aerated filtered cement solution (with Aquadem<sup>®</sup>, diagrams plotted at  $E_{\text{cor}}$ ).

contact with the mortar, with and without Aquadem<sup>®</sup>. The results shown in Figures 5 and 6 with Aquadem<sup>®</sup> were compared to those obtained with an E24 steel RDE at 0 rpm, after 1 h of immersion in an aerated filtered cement solution. The results were found to be independent of the presence or absence of Aquadem<sup>®</sup>.

The current–potential curves and the impedance diagrams obtained in the mortar are similar to those obtained in the filtered cement solution, and in particular, the anodic plateau currents are the same ( $0.8 \mu\text{A cm}^{-2}$ ). In the case of the mortar, the film capacitance calculated from the high frequency part of the impedance diagram is equal to  $0.5 \mu\text{F cm}^{-2}$ , which is about 20 times lower than the values assessed for the filtered cement solution. This means that for the experiments in the mortar, the passive film is much thicker than for the filtered cement solution.

Thus, the E24 steel in contact with a mortar enclosing no large air cavity is passivated as well as in a filtered cement solution. Therefore the presence of the solid phase in the electrolyte is not responsible for the localized corrosion observed in service conditions.

#### 4. Conclusions

In a filtered cement solution, the E24 steel is passivated, with or without Aquadem<sup>®</sup>, and the corrosion mechanism is totally controlled by the anodic process and not by oxygen reduction. Whatever the experimental conditions (rotation speed,  $\text{O}_2$  concentration, presence or absence of Aquadem<sup>®</sup>), the corrosion current,  $i_{\text{cor}}$ , equals the anodic plateau current,  $i_{\text{plateau}}^{\text{a}}$ , and is of the order of  $0.8 \mu\text{A cm}^{-2}$ . Therefore, it has been demonstrated that  $i_{\text{cor}}$  may be directly assessed from the steady state current–potential curves.

The E24 steel in contact with a homogeneous mortar without large air cavities is passivated as well as in a filtered cement solution. Therefore, the pitting corrosion observed in service conditions does not arise from the presence of a solid phase in the electrolyte, but may result from the heterogeneity of the concrete due to air cavities.

Thus, the pitting corrosion observed in service conditions would probably be avoided if the concrete was poured in the moulds without formation of large air cavities. However, so as to understand the mechanism of localized corrosion, the next step in our work will be to study the behaviour of the E24 steel in contact with a heterogeneous mortar containing large air cavities (i.e., in contact with the gas–liquid–solid threephase electrolyte) and to understand how the presence of these cavities can lead to passive film breakdown.

#### References

1. J. Bresson, *CERIB Fiche* **118** (1996) 563.
2. C. Andrade, in 'Matériaux et Constructions', RILEM, Vol. 29 (1996), pp. 40–46, 97–104.
3. G. Song and A. Shayan, ARRB Transport Research Ltd, Review Report 4, July (1998).
4. J. Kissel and A. Pourbaix, in Proceedings Eurocorr 2000, London, Sept. (2000).
5. M. Mosquet, Thesis, University Claude Bernard, Lyon I, France (1994).
6. K.J. Vetter, *Elektrochem.* **58** (1954) 230.
7. M. Pourbaix, 'Atlas d'Equilibres Electrochimiques' (Gauthier Villard & Cie, Paris, 1966).
8. V.G. Levich, 'Physicochemical Hydrodynamics' (Prentice Hall, Englewood Cliffs, NJ, 1962), p. 72.
9. E.J. Calvo and D.J. Schiffrin, *J. Electroanal. Chem.* **243** (1988) 171.
10. N. Le Bozec, C. Compère, M. L'Her, A. Laouenan, D. Costa and P. Marcus, *Corros. Sci.* **43** (2001) 765.
11. S. Haupt and H.H. Strehblow, *Langmuir* **3** (1987) 873.